Materials Research Proceedings **5** (2018) 154-159 doi: http://dx.doi.org/10.21741/9781945291814-27

Enhanced Surfaces Used in Research on Flow Boiling Heat Transfer in Minichannels

STRĄK Kinga[1, a *], PIASECKA Magdalena[2,b] and STRĄK Dariusz[3,c]

[1,2,3] Kielce University of Technology, Al. Tysiaclecia Panstwa Polskiego 7, 25-314 Kielce, Poland

[a]kzietala@tu.kielce.pl, [b]tmpmj@tu.kielce.pl, [c]dstrak@tu.kielce.pl

Keywords: Laser Texturing, Vibration-Assisted Laser Texturing, Electromachining Texturing, Porous Surface, Flow Boiling, Heat Transfer, Minichannel

Abstract. This paper reviews enhanced surfaces used to study boiling heat transfer in minichan-nels with rectangular cross-sections. Experiments were conducted for refrigerants flowing along a vertical minichannel, asymmetrically heated by one of the enhanced surfaces. The enhanced surfaces used in the experiments were the following: laser textured and vibration-assisted laser textured surfaces with regular cavities, electro-discharge machined surfaces with irregular cavities, fibrous surfaces with capillary-porous structures, and powder-coated surfaces. Heat transfer efficiency was evaluated based on local heat transfer coefficients calculated at the heated surface-fluid interface in the minichannel. Vibration-assisted laser surface texturing provided the most efficient heat transfer compared to the other enhanced surfaces and the smooth surface.

Introduction

The current trend towards miniaturization has accelerated the development of heat transfer solutions for energy supply and cooling of heat-generating machine components. Effective cooling methods employ heat transfer processes accompanied by a phase change. The heat transfer coefficients obtained during these processes are higher than those provided by forced convection heat transfer without a phase change. One of the methods of heat transfer enhancement involves heat transfer surface modification. The modification causes the increase of heat transfer coefficient values through increasing the number of active nucleation sites during flow boiling [1-10] or pool boiling [10-12]. Modified surfaces exhibit reduced surface superheating and improve heat dissipation by increasing the area of heat removal. Heat exchangers with enhanced surfaces find application over a wide range of industries from microelectronics (cooling of large scale integrated circuits, microprocessors, memory modules) to power engineering (gas micro turbines). The literature describes numerous processes that are used to modify metallic surfaces [13-16]. In their previous articles, the authors of this paper reported their findings concerning various enhanced heat transfer surfaces with the flow of various working fluids through rectangular heat exchangers with minichannels. The surfaces studied included laser-textured surfaces with regular recesses [2,7], vibration-assisted laser-textured surfaces [3,4,6], surfaces with irregular recesses obtained in the process of spark erosion [1,2,5,6,10,11], surface with capillary-fibrous structure [1] and powder surfaces produced by sintering or soldering [8,9]. Based on the research results for flow boiling in minichannels, this article discusses the enhanced surfaces used, along with their production methods and effects on heat transfer processes.

Characteristics of smooth surface (base)

All the enhanced heated plates were made on smooth plate (base) with a Haynes-230 alloy plate, about 0.10 mm and 0.45 mm thick or a Hastelloy X alloy plate, about 0.65 mm thick. All the tested alloy plates were manufactured by Haynes Int. Inc. (USA) and chosen for their electrical resistivity, assuming minor resistivity changes with temperature. The Hastelloy X and Haynes-230 alloy plates are made mainly of Ni-Cr-Fe-Mo and Ni-Cr-W-Mo alloys, respectively. In addition to excellent

high-temperature strength and oxidation resistance [6]. Images of the smooth and enhanced tested surfaces were presented in Fig. 1.

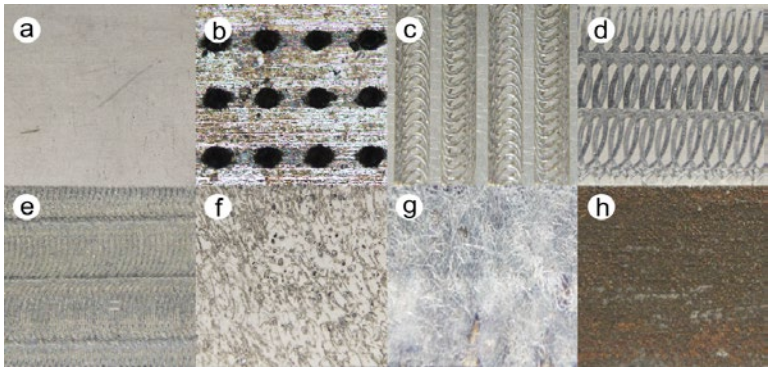

Fig. 1. Images of the tested surfaces: a) smooth, b) laser surface texturing, c-e) vibration-assisted laser texturing no: 1 (c), 2 (d), 3 (e), f) electromachining texturing, g) capillary-fibrous structure, h) porous structure produced by Fe powder soldering

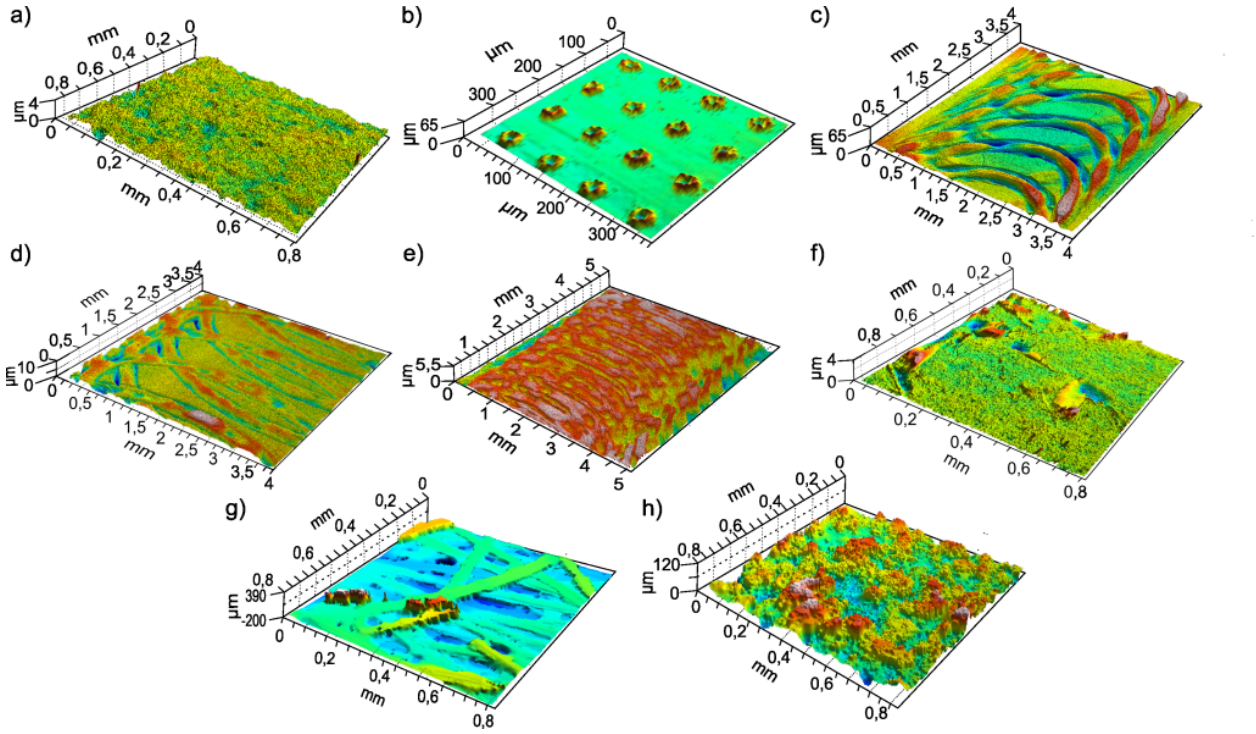

Fig.2. Fragment of 3D surface topography: (a) smooth, b) laser surface texturing, c-e) vibration-assisted laser texturing: 1 (c), 2 (d), 3 (e), (f) electromachining texturing, g) capillary-fibrous structure, h) porous structure-produced by Fe powder soldering

Table 1. The arithmetic mean height (Sa) and arithmetic mean deviation of the roughness profile (Ra) of the tested plate

Parameter	Types of surface						
[µm]	smooth	vibration-assisted laser 1	vibration-assisted laser 2	vibration-assisted laser 3	electro-machining	capillary-fibrous structure	porous, produced by soldering
Sa	0.346	7.934	1.981	3.589	0.983	41.044	13.919
Ra	0.175	3.812	1.364	1.025	0.615	21.407	11.283

The study of roughness parameters was conducted at the Geometric Computer Measurement Laboratory at the Kielce University of Technology. The profilometer measured using the Taylor

Hobson CCI to ISO 25178-2:2012 enables measurement and analysis of the geometric structure of the tested surface (Tab. 1).

Characteristics of surfaces with laser and vibration-assisted laser surface texturing

During the laser microprocessing, the material is removed by the laser beam's energy. An impulse beam time depends on the radiation intensity and exposure time. The cavities on the surface were performed with a laser drilling with a diode pumped Nd:YAG laser producing UV radiation of the wavelength of 355 nm and were evenly distributed every 100 μm in both axes. One of four tested enhanced surfaces [2] produced on the 0.10 mm thick Haynes plate had the best properties in terms of heat transfer, Fig. 2b. The diameter of a single cavity had 10 μm, its depth was 3 μm, 5-7 μm high layers of melted metal deposited annularly around the cavities, forming structures as "craters" [2, 7].

One Hastelloy X alloy (0.65 mm thick) surface and two Haynes-230 alloy (0.45 mm thick) surfaces processed using the vibration-assisted laser surface texturing were studied. The surfaces were prepared with the CO_2 Trumpf Lasercell 1005 owned by the Centre for Laser Technologies of Metals at the Kielce University of Technology. The Hastelloy X alloy surface, surface no 1, (Fig. 2c) had the laser paths aligned perpendicularly to the flow in the minichannel [6]. The texturing process followed the programmed trajectory of the laser head movement with the following processing parameters: laser power of 2500 W, scanning velocity of 4 m/min, and argon blow intensity of 10 l/min.

The two other vibration-assisted laser surfaces were made of the Haynes-230 alloy (0.45 mm thick) and had the laser paths arranged along the flow, with a lower laser path density in the case of surface no 2 (Fig. 2d) and a higher laser path density in the case of surface no 3 (Fig. 2e). The processing parameters for these surfaces were as follows: laser power of 1500 W or 1250 W, scanning velocity of 4 or 2 m/min, and argon blow intensity of 10 l/min [3, 4].

Characteristics of the surface with electromachining texturing

During the spark erosion process in electromachining, the eroded material is transferred from the anode to the cathode. As a result, the cathode surface is covered with pure anode material or a layer created by the mutual impacts between electrodes and the medium between electrodes. The intensity of the transfer of the material depends mainly on impulse energy [2, 9]. Sample cavities in the 0.10 mm thick Haynes-230 alloy surface section were made by electromachining, using an electric-etcher and branding-pen manually controlled and oriented in selected directions. Finally, one method was selected to produce cavities (Fig. 2f). The depth of the cavity craters was usually below 2 μm. The layer of melted metal of the plate and the electrode material, a few μm high, reaching locally 5 μm, accumulated around the cavities.

Characteristics of the surface with the capillary-fibrous structure

The surface with the capillary-fibrous structure was soldered to the 0.1 mm thick Haynes-230 plate surface, manufactured using stainless steel fibers 0.1 mm in thickness and about 2 cm in height. The length of the capillary structure, see figure 2.b (III), was usually up to 2 cm. They were spot welded with a microwelder and rolled to a thickness of 0.15 – 0.2 mm (Fig. 2g) [1].

Characteristics of the porous surface produced by soldering and sintering iron powder

The porous surface was produced by soldering to the tested surface (made of the Haynes-230) according to the method described in the Polish patent [17]. The main parameters of the microstructured surface are the following: the diameter of a solder granule - approx. 15÷80 μm (with an average being 40÷65 μm), the density of the solder paste – 2990 kg/m^3, the thickness of the soldered layer – approx. 100 μm and its maximum height – 200 μm (Fig. 2h). One of the porous surface types was produced with metal foams formed by the reduction of metal oxides during sintering. The mixture was sintered in a dissociated ammonia atmosphere. The iron foam was

prepared according to the method described in the Polish patent [18]. The porous layers were formed by the sintering technique, the powder mixture and the reduction of iron powder ASC 100.29, ASC 100.24, DISTALOY SE and iron oxide of different granulation. The powder mixture was sintered in a dissociated ammonia atmosphere at 1180 ^{o}C for 45 minutes.

Experimental stand and the heat transfer coefficient calculation

The experimental stand (Fig. 3) is composed of several systems: the test loop in which Fluorinert FC-72 circulates as the working fluid, the calibration loop, the data and image acquisition system, the supply and control system and the lighting system, described in [4]. Local heat transfer coefficients were determined using the one-dimensional method, presented in [4, 5].

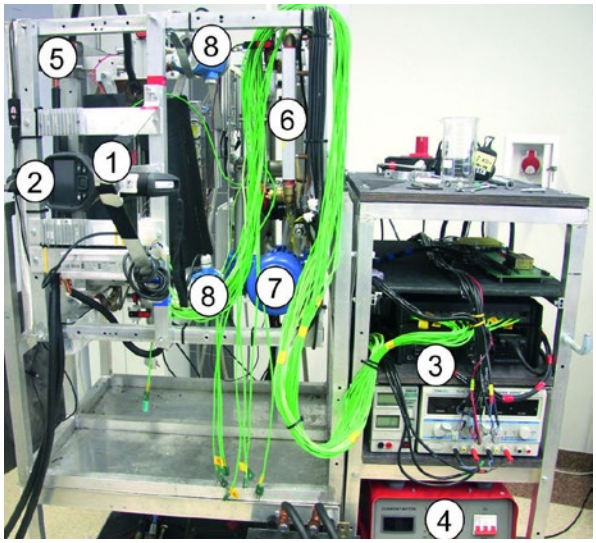

Fig. 3. The image of the main systems of the experimental setup, with visible elements marked: 1 - test section, 2 - infrared camera, 3 - data acquisition station, 4 - inverter welder, 5 - shunt, 6 - mass flowmeter, 7 - gear pump, 8 - pressure sensor

Results

The results confirm that considerable heat transfer enhancement takes place when selected enhanced heated surface is used in the minichannel flow boiling and that it depends on the type of surface enhancement. The analysis of the experimental data revealed that the values and distributions of the heat transfer coefficient (α) versus the distance from the minichannel inlet (x). The experiments were conducted using the test module with Fluorinert FC-72 flow along the minichannel 1.7 mm deep, 16 mm wide, and 180 mm long, vertically oriented [6].

Figure 4 shows examples of the results represented as the heat transfer coefficient vs. the distance from the minichannel inlet obtained for the surface with the vibration assisted laser surface texturing no 2 and the surface with the capillary-fibrous structure.

The results for all the surfaces used in the experiments indicated that:

- the surfaces with the vibration assisted laser surface texturing no 2 provided the highest values of the heat transfer coefficient, which could be due to the laser path alignment along the fluid flow in the minichannel and lower density of the laser path leading to more intense formation of nucleation sites,
- the surface with the capillary-fibrous structure showed the lowest values of the heat transfer coefficient, probably due to the instability of the boiling fluid flow and its turbulization.

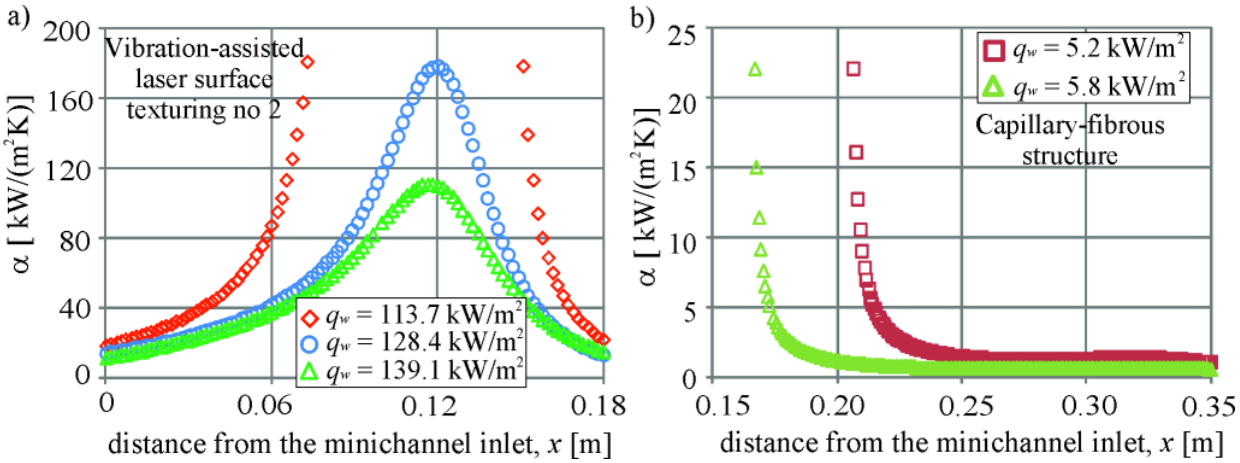

Fig. 4. Heat transfer coefficient vs. the distance from the minichannel inlet: a) surface no 2 with vibration assisted laser surface texturing, data for the saturated boiling region, experimental parameters: average inlet pressure p_{in} = 161 kPa, average mass flux G = 440 kg/(m²s), average inlet liquid subcooling ΔTsub = 45 K, b) surface with capillary-fibrous structure; experimental parameters: average inlet pressure p_{in} = 118 kPa, average mass flux G = 161 kg/(m²s), average inlet liquid subcooling ΔTsub = 42 K

Conclusions

This paper reports the test results for FC-72 flow boiling heat transfer in a vertical, asymmetrically heated minichannel with different surface modifications.

The heat transfer efficiency was evaluated on the basis of heat transfer coefficient values at the interface between the enhanced heating surface and the cooling liquid flowing through the minichannel. The laser-vibration-assisted texturing surface no 2 provided the most effective heat transfer. Compared to the other analyzed surfaces, the lowest coefficients were provided by the surface with the capillary-fibrous structure.

It can be concluded that the application of the enhanced surfaces allows achieving effective heat transfer. The enhanced surfaces can be successfully applied to compact heat exchangers with minichannels.

Acknowledgments

The research reported herein was supported by a grant from the National Science Centre, Poland (No DEC-2016/23/N/ST8/01247).

References

[1] M. Piasecka, K. Strąk, Effect of the heating surface enhancement on the heat transfer coefficient for a vertical minichannel, EPJ Web of Conferences 114, 02095 (2016). https://doi.org/10.1051/epjconf/201611402095

[2] M. Piasecka, Laser texturing, spark erosion and sanding of the surfaces and their practical applications in heat exchange devices, Adv. Mater. Res. 874 (2014) 95–100. https://doi.org/10.4028/www.scientific.net/AMR.874.95

[3] K. Strąk, M. Piasecka, B. Maciejewska, B. Grabas, A study of the flow boiling heat transfer in a minichannel for a heated wall with surface texture produced by vibration-assisted laser

machining, J. Phys. Conf. Ser. 745, 32123 (2016). https://doi.org/10.1088/1742-6596/745/3/032123

[4] K. Strąk, M. Piasecka, B. Maciejewska, Spatial orientation as a factor in flow boiling heat transfer of cooling liquids in enhanced surface minichannels, Int. J. Heat Mass Transf. 117 (2018) 375–387. https://doi.org/10.1016/j.ijheatmasstransfer.2017.10.019

[5] M. Piasecka, K. Strąk, B. Maciejewska, Calculations of flow boiling heat transfer in a minichannel based on liquid crystal and infrared thermography data, Heat Transf. Eng. 38(3) (2017) 332–346. https://doi.org/10.1080/01457632.2016.1189272

[6] M. Piasecka, K. Strąk, B. Grabas, Vibration-assisted laser surface texturing and electromachining for the intensification of boiling heat transfer in a minichannel, Arch. Metall. Mater. 62(4) (2017) 1983–1990. https://doi.org/10.1515/amm-2017-0296

[7] M. Piasecka, Flow boiling heat transfer in a minichannel with enhanced heating surface, Heat Transf. Eng. 35 (10) (2014) 903–912. https://doi.org/10.1080/01457632.2014.859505

[8] B. Maciejewska, K. Strąk, M. Piasecka, The solution of a two-dimensional inverse heat transfer problem using the Trefftz method, Procedia Eng. 157 (2016) 82–88. https://doi.org/10.1016/j.proeng.2016.08.341

[9] W. Depczyński, A. Piasecki, M. Piasecka, K. Strąk, Impact of Fe powder sintering and soldering in production of porous heating surface on flow boiling heat transfer in minichannels, E3S Web of Conferences 19, 03012 (2017), 1-6.

[10] M. Piasecka, Heat transfer research on enhanced heating surfaces in flow boiling in a minichannel and pool boiling, Ann. Nucl. Energy. 73(2014) 282-293. https://doi.org/10.1016/j.anucene.2014.06.041

[11] R. Pastuszko, M. Piasecka, Pool boiling on surfaces with mini-fins and micro-cavities, J. Phys. Conf. Ser. 395, 012137 (2012). https://doi.org/10.1088/1742-6596/395/1/012137

[12] R. Kaniowski, R. Pastuszko, Ł. Nowakowski, Effect of geometrical parameters of open microchannel surfaces on pool boiling heat transfer, EPJ Web of Conferences 143, 02049 (2017). https://doi.org/10.1051/epjconf/201714302049

[13] W. Depczyński, Kazala R., Ludwinek K., Jedynak K., Modelling and microstructural characterization of sintered metallic porous materials, Materials 9 (7), 567 (2016). https://doi.org/10.3390/ma9070567

[14] N. Radek, J. Konstanty, Cermet ESD coatings modified by laser treatment, Arch. Metall. Mater. 57 (2012) 665-670. https://doi.org/10.2478/v10172-012-0071-y

[15] N. Radek, J. Pietraszek, B. Antoszewski, The average friction coefficient of laser textured surfaces of silicon carbide identified by RSM methodology, Adv. Mat. Res. 874 (2014) 29-34. https://doi.org/10.4028/www.scientific.net/AMR.874.29

[16] J. Borowiecka-Jamrozek, J. Lachowski, Modelling of retention of a diamond particle in matrices based on Fe and Cu, Procedia Eng. 177 (2017) 289-296. https://doi.org/10.1016/j.proeng.2017.02.227

[17] M. Piasecka, PL. Patent 225512 B1, dec. (2016).

[18] W. Żórawski. R. Chatys, W. Depczyński, PL. Patent 199720 B1, dec. 2008.